Journal of Alloys and Compounds 512 (2012) 179–184

Contents lists available at SciVerse ScienceDirect

Journal of Alloys and Compounds

journal homepage: www.elsevier.com/locate/jallcom

Investigation of the effective parameters on the synthesis of strontium hexaferrite nanoparticles by chemical coprecipitation method

A. Davoodi*, B. Hashemi

Department of Materials Science and Engineering, School of Engineering, Shiraz University, Zand Street, Shiraz, Iran

ARTICLE INFO

Article history:
Received 19 August 2011
Received in revised form
17 September 2011
Accepted 19 September 2011
Available online 24 September 2011

Keywords:
Nanostructured materials
Chemical synthesis
Magnetic measurements
Permanent magnets

ABSTRACT

Strontium hexaferrite nanoparticles were synthesized by chemical coprecipitation method in the presence of polyvinylpyrrolidone (PVP) as a protective agent. A mixture of the deionized water/ethanol (50/50) was used as the solvent. The effects of PVP, pH of the solution, Fe^{3+}/Sr^{2+} molar ratio and calcination temperature of the precipitates on the synthesis of strontium hexaferrite samples were studied. X-ray diffraction (XRD), scanning electron microscope (SEM), thermal analysis (DTA–TGA), dynamic light scattering particle size analyzer (PSA) and vibrating sample magnetometer (VSM) were used to investigate the properties of the obtained samples. The results showed that increasing the pH from 9 to 13 or decreasing Fe^{3+}/Sr^{2+} molar ratio from 12 to 9 promoted $SrFe_{12}O_{19}$ formation and decreased the size of nanoparticles. The minimum coercivity of 4733 Oe and maximum saturation magnetization of 51 emu/g were obtained by increasing the pH from 9 to 13. It was also concluded that PVP could be effective in decreasing the size of $SrFe_{12}O_{19}$ nanoparticles and resulted to decrease the calcination temperature from 800 to 700 °C.

1. Introduction

Strontium hexaferrite due to relatively low price, high Curie temperature, high coercivity and excellent chemical stability has significant potential for applications such as permanent magnets, microwave absorbing materials and magneto-optical devices [1,2]. The conventional method for the synthesis of hexaferrites involves solid-state reaction of strontium carbonate and iron oxide mixtures at high temperature (~1200 °C) [3]. However, chemically homogeneous strontium hexaferrite with very fine particles, narrow particle size distribution and good magnetic properties is required for specific applications while these are not obtainable by the conventional method [4,5]. In order to overcome these disadvantages, various methods such as hydrothermal [6,7], microemulsion [8], sol–gel [9–11], glass crystallization [12] and coprecipitation [13–16] have been investigated. Coprecipitation is a simple and low cost method for the synthesis of strontium hexaferrite [15]. Nevertheless, the preparation of the mono-dispersed nanoparticles may not be easy. The influence of some effective parameters such as Fe^{3+}/Sr^{2+} molar ratio on the synthesis of $SrFe_{12}O_{19}$ have been reported, where water was used as the solvent [17]. The use of a mixed solvent and addition of a soluble polymer to solvent is a new approach in order to synthesize the nanoparticles and control the nucleation and growth of them. The strontium hexaferrite nanoparticles have been synthesized in the presence of polyacrylic acid (PAA) as a protective agent in an aqueous solution [18]. Synthesis of coprecipitated strontium hexaferrite nanoparticles in the presence of polyvinyl alcohol (PVA) has been reported in a previous paper [19]. The recent research aims to study the effects of Fe^{3+}/Sr^{2+} molar ratio, pH of the solution, calcination temperature of the precipitates and addition of PVP (as a protective agent), on the synthesis and magnetic properties of strontium hexaferrite nanoparticles via coprecipitation method.

2. Experimental

High purity raw materials, Fe $(NO_3)_3 \cdot 9H_2O$ (Merck, >99%), $Sr(NO_3)_2$ (Merck, >99%) and NaOH (Merck, >99%) were used as starting materials. The iron and strontium nitrates with the Fe^{3+}/Sr^{2+} molar ratios of 9 up to 12 were dissolved in mixture of deionized water/ethanol (50/50, vol%) as the solvent. Then an equal volume of 1 wt% PVP $(C_6H_9NO)_n$ solution was added to some solutions as protective agent. The prepared solutions were co-precipitated at pH values of 9–13 by addition of NaOH solution (2 M). The separation of the precipitates from solutions was done by nano-filter paper or sedimentation method. In the first method the precipitates were filtered by nano-filter paper and washed several times, using deionized water until the pH value of the solution became neutral. In the second method, solid particles were separated from the solution by sedimentation of the particles and suction of the above liquid into another container, without disturbing the precipitates. The precipitates after drying at 80 °C were calcined at various temperatures for 2 h. The phase composition was determined by X-ray diffraction (XRD). A Bruker, D8 advanced X-ray diffractometer with Cu K_α radiation was used. A Leica Cambridge, S360 scanning electron microscope (SEM) and dynamic light scattering nanoparticle size analyzer (Horiba LB-550) were used to characterize the particle size. Thermal behavior of the samples was examined by simultaneous differential thermal

* Corresponding author. Tel.: +98 7116133399; fax: +98 7112307293.
E-mail address: akbardavudijamaloee@yahoo.com (A. Davoodi).

0925-8388/$ – see front matter © 2011 Elsevier B.V. All rights reserved.
doi:10.1016/j.jallcom.2011.09.059

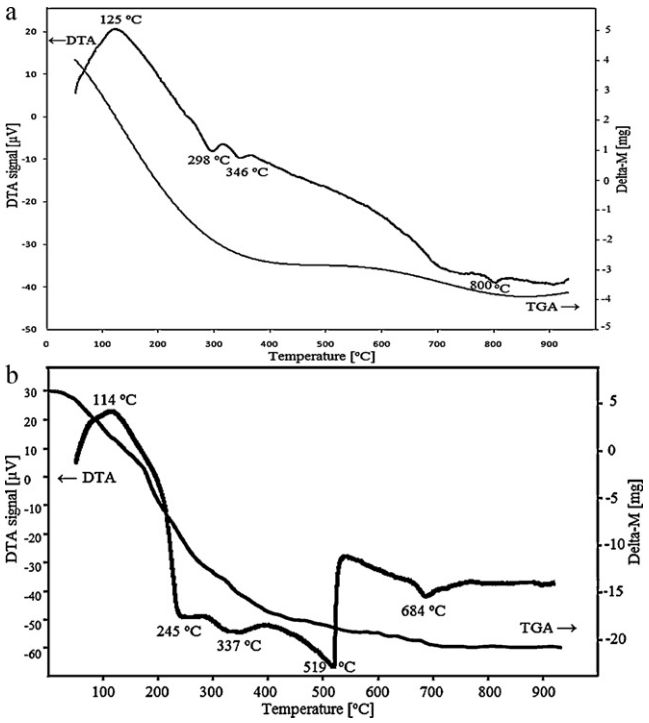

Fig. 1. DTA–TGA curves of the precursors obtained at Fe^{3+}/Sr^{2+} = 9 and pH = 13, in the absence (a) and presence of PVP (b), separated by filtration method.

and thermo-gravimetric analyses (DTA–TGA, Linseis L81) with a heating rate of 10 °C/min. The magnetic properties were measured using a VSM with maximum field strength of 1 T (10000 Oe).

3. Results and discussion

The TGA and DTA curves for the precursor obtained at Fe^{3+}/Sr^{2+} molar ratio of 9, pH = 13 and without and with PVP are shown in Fig. 1. The TGA curve in Fig. 1(a) shows the weight loss of the sample without PVP up to 800 °C. The high weight loss from room temperature to about 250 °C is because of the loss of the residual water in the sample. The weight loss of the sample from 250 to 400 °C may be due to conversion of hydroxides to oxides. The weight of the sample remains constant between 400 and 550 °C. The formation of $SrFe_{12}O_{19}$ causes a small weight loss after 550 °C. The DTA curve exhibits a broad endothermic peak at around 125 °C and three exothermic peaks at 298, 346 and 800 °C. The endothermic peak is due to the loss of the residual water. Two exothermic peaks at 298 and 346 °C could be related to the conversion of hydroxides to oxides [19,20]. The exothermic peak at 800 °C probably attributes to the formation of $SrFe_{12}O_{19}$. Fig. 1(b) shows the TGA and DTA curves of the sample in the presence of PVP. The TGA curve behavior is similar to previous sample but higher weight loss exists due to the burning of PVP. No weight change is seen after 700 °C. A broad endothermic peak around 114 °C and four exothermic peaks at 245, 337, 519 and 684 °C are observed in DTA curve. The exothermic peak reveals around 519 °C may be resulted from the burning of the PVP. The other peaks are the same as the previous sample, but occur at the lower temperatures. It can be concluded that using PVP reduces the formation temperature of strontium hexaferrite.

Fig. 2 shows the X-ray diffraction patterns of the samples prepared with different pH values (9, 11 and 13) and Fe^{3+}/Sr^{2+} molar ratio of 12 after calcination at 750 °C for 2 h. As seen, the sample obtained at pH = 9 is a mixture of Fe_2O_3 and $SrFe_{12}O_{19}$ phases but Fe_2O_3 peaks are very weak at pH = 13. It indicates that the $SrFe_{12}O_{19}$ formation is promoted by increasing the pH. Therefore pH = 13 was selected as optimum pH. The presence of the small amount of Fe_2O_3

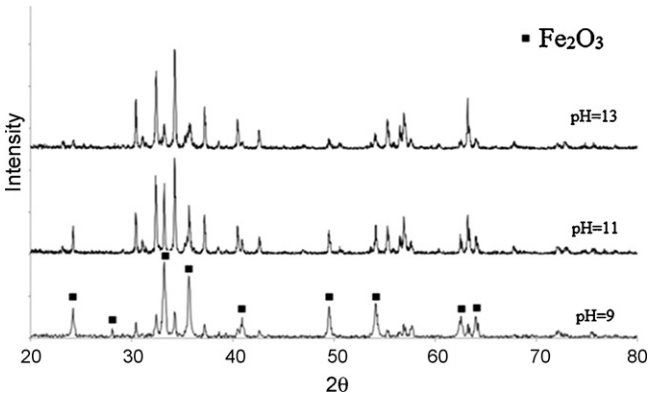

Fig. 2. X-ray diffraction patterns of the samples, precipitated at different pH values with Fe^{3+}/Sr^{2+} = 12, separated by filtration method and calcined at 750 °C for 2 h.

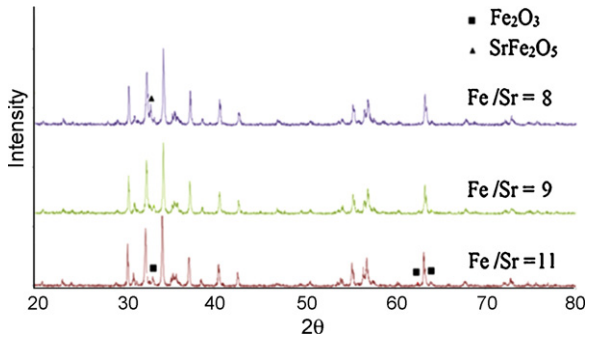

Fig. 3. X-ray diffraction patterns of the samples obtained at different Fe^{3+}/Sr^{2+} molar ratios and pH = 13, separated by filtration method, after calcination at 750 °C for 2 h.

at pH = 13 is related to lack of strontium. Because the strontium hydroxide has few solubility in solvent therefore an excess amount of Sr^{2+} relative to stoichiometric ratio is required to react with Fe^{3+} [18].

The influence of Fe^{3+}/Sr^{2+} molar ratio on the phase composition of the samples calcined at 750 °C is shown in Fig. 3. The X-ray diffraction patterns show that the $SrFe_{12}O_{19}$ content is increased by decreasing the Fe^{3+}/Sr^{2+} molar ratio from 11 to 9 and it confirms the above argument. Decreasing the molar ratio to 8 and lower values led to formation of $SrFe_2O_5$ due to excess amount of strontium in the system. The obtained results are comparable with those reported earlier [17].

The X-ray diffraction pattern of the sample with 1 wt% PVP (calcined at 700 °C) is shown in Fig. 4. All of the peaks are corresponding with $SrFe_{12}O_{19}$ phase and peaks of the other phases are not seen. According to TGA results, the addition of PVP effectively decreases the formation temperature of strontium hexaferrite. This is because

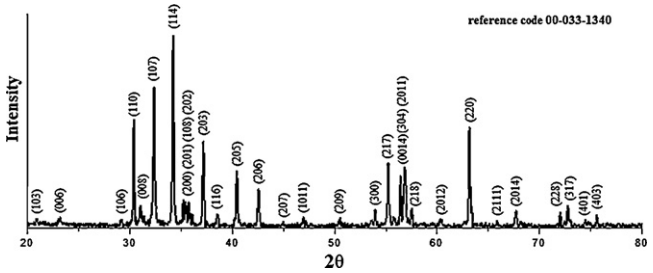

Fig. 4. X-ray diffraction pattern of the sample synthesized in the presence of PVP at pH = 13 and Fe^{3+}/Sr^{2+} = 9, separated by filtration method, after calcination at 700 °C for 2 h.

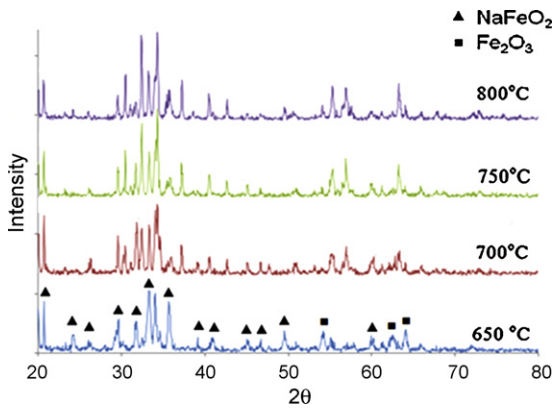

Fig. 5. X-ray diffraction patterns of the precipitates separated by sedimentation method, at pH = 13 and Fe^{3+}/Sr^{2+} = 9 after calcination at various temperatures.

of the smaller particle size of the precipitates and will be discussed in the following.

The effect of the separation method of the precipitates from the solution on the phase composition of the samples was shown in Fig. 5. It show, the X-ray diffraction patterns of the samples precipitated by sedimentation method, which were calcined at different temperatures (650, 700, 750 and 800 °C). As seen, increasing the calcination temperature enhances the formation of $SrFe_{12}O_{19}$. Nevertheless, in comparison with the obtained results for the precipitates separated by the filtration method, all of the samples are mixture of $SrFe_{12}O_{19}$, $NaFeO_2$ and Fe_2O_3 phases. Existence of sodium phases in X-ray analysis indicates that sedimentation method cannot be an effective method for separation of $SrFe_{12}O_{19}$ precipitates from solution.

The SEM micrographs of the obtained precursors at various pH values were shown in Fig. 6. An image analyzer was used to measure the mean particle size of the samples. The mean particle size of the precursors with pH 9, 10, 12 and 13 were 81, 69, 47 and 35 nm, respectively. The results show that the mean particle size of the precursors decreases by increasing the pH from 9 to 13. The addition of NaOH to solution increases the pH value (OH^- concentration) and causes the cations (Fe^{3+} and Sr^{2+}) to react with the anion (OH^-). Therefore, pH value is effective on reaction rates and enhances nucleation rate of the precursors. In other words, increase in the pH value encourages a burst of nucleation and decreases growth.

Fig. 7 shows the size distributions of the previous samples (obtained at various pH) after calcination at 800 °C for 2 h. The average particle sizes of the samples were 97, 90, 84 and 75 nm in order of increasing the pH. The increase in particle size may be due to calcination or aggregation of particles during testing. Similar results have been reported by Janasi et al. [21].

The effect of the Fe^{3+}/Sr^{2+} molar ratio on the particle size was studied by the SEM micrographs (Fig. 8). From the images, it is evident that the average particle size decreases by decreasing of Fe^{3+}/Sr^{2+} molar ratio. The average particle size of the ferrites prepared with Fe^{3+}/Sr^{2+} molar ratios of 11, 10 and 8 were 103, 85 and 73 nm, respectively.

The particle size of the sample containing PVP with Fe^{3+}/Sr^{2+} = 9 and pH = 13 was analyzed by SEM and PSA (Figs. 9 and 10). The results show that PVP reduces the average particle size of the sample. The average particle size of the synthesized strontium

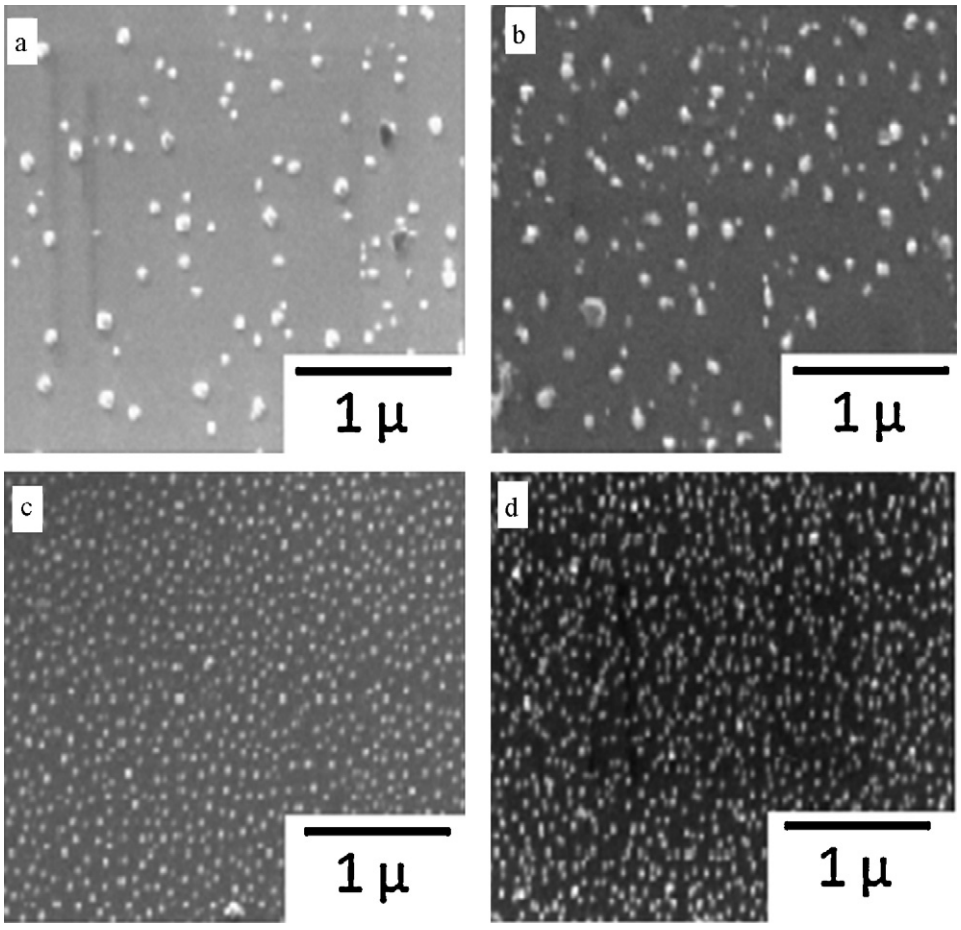

Fig. 6. SEM micrographs of the precursors separated by filteration method with Fe^{3+}/Sr^{2+} = 9, precipitated at (a) pH = 9, (b) pH = 10, (c) pH = 12 and (d) pH = 13.

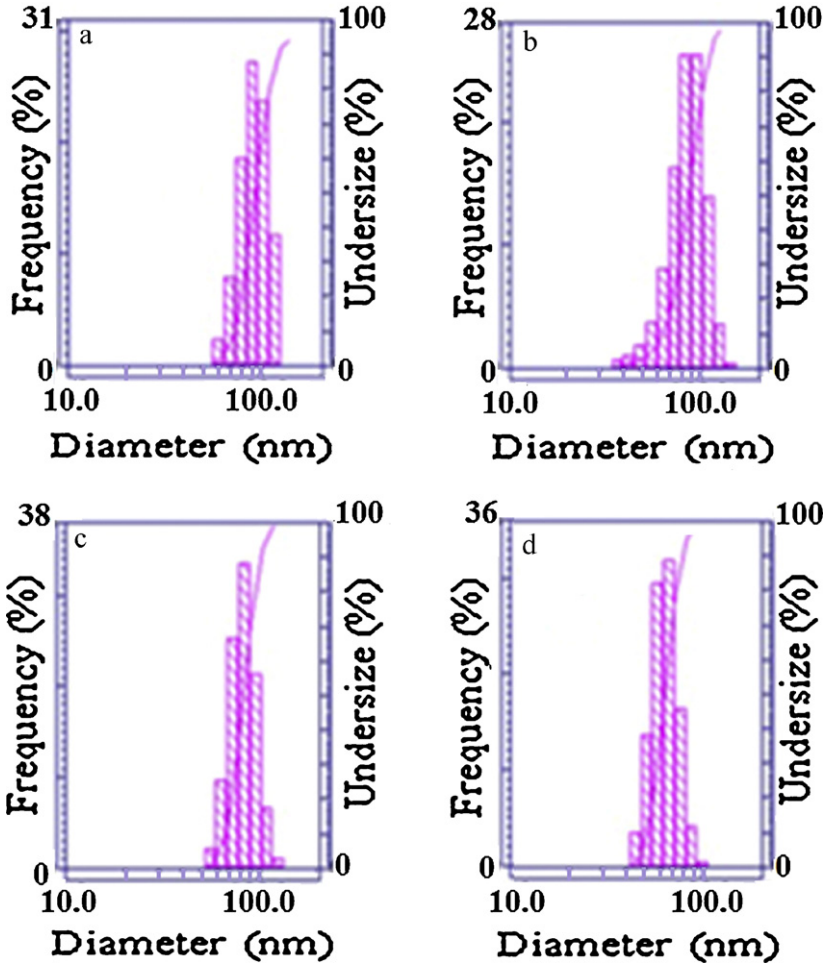

Fig. 7. Particle size distribution of the samples with Fe^{3+}/Sr^{2+} = 9, precipitated at (a) pH = 9, (b) pH = 10, (c) pH = 12 and (d) pH = 13, separated by filteration method, after calcination at 800 °C for 2 h.

hexaferrite with 1 wt% PVP as a protective agent was 24 and 59 nm before and after calcination at 700 °C for 2 h, respectively. Surfactants or polymers were often adsorbed by the surface of the particles during or after the synthesis of them and avoid from agglomeration. The adsorbed PVP molecules provides a passive layer on the surface of particles that its electrostatic or steric repulsions would provide stability of the dispersed nanoparticles and prevents the growth or agglomeration of them.

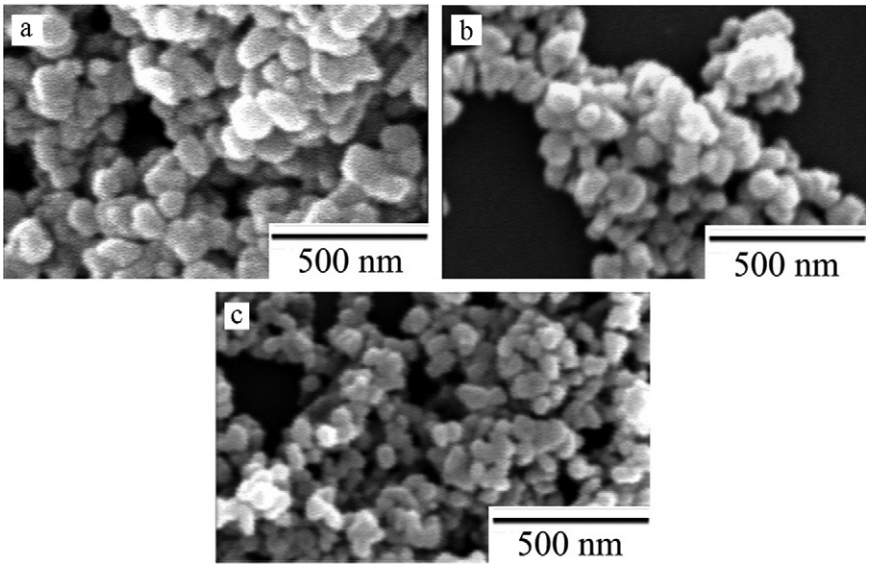

Fig. 8. SEM micrographs of the samples prepared at pH = 13 with Fe^{3+}/Sr^{2+} = 11 (a), Fe^{3+}/Sr^{2+} = 10 (b) and Fe^{3+}/Sr^{2+} = 8 (c), separated by filteration method and calcined at 800 °C for 2 h.

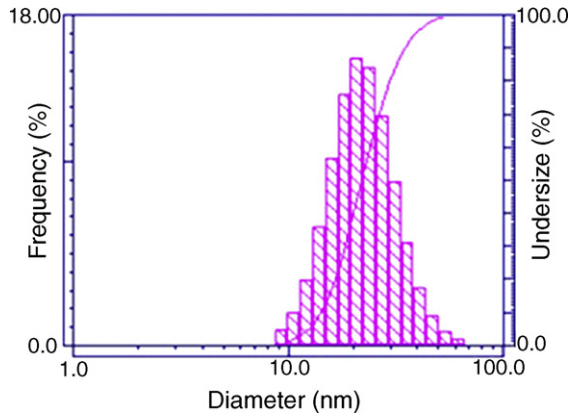

Fig. 9. Particle size distribution of the precursor otained in the presence of 1 wt% PVP at pH = 13 and Fe^{3+}/Sr^{2+} = 9, separated by filteration method.

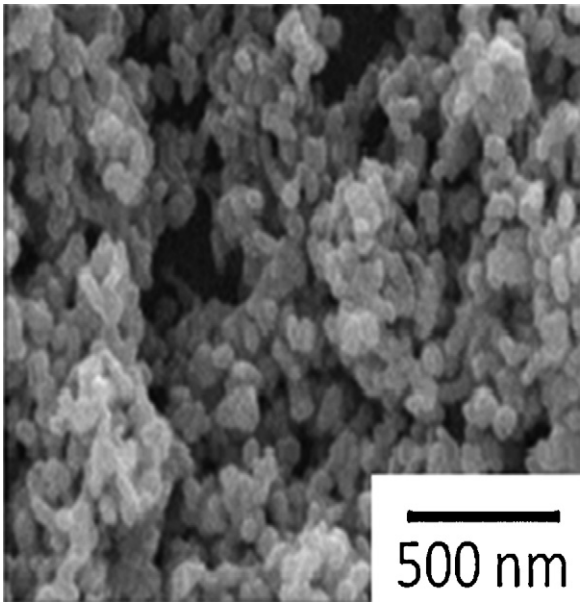

Fig. 10. SEM micrograph of the sample separated by filteration method and synthesized in the presence of 1 wt% PVP, pH = 13 and Fe^{3+}/Sr^{2+} = 9 after calcination at 700 °C for 2 h.

The magnetic properties of the samples with different pH, Fe^{3+}/Sr^{2+} = 9 and calcined at 750 °C are shown in Fig. 11 and Table 1. The coercivity decreases by increasing the pH from 9 to 13. Below a critical diameter D_s the particles become single domains, and in this size range the coercivity decreases as the particle size decreases, because of thermal effects, according to following relation:

$$H_{ci} = g\left(\frac{h}{D^{3/2}}\right) \quad (1)$$

where H_{ci} is intrinsic coercivity, g and h are constant values and D is particle diameter [22]. Therefore decreasing particle size is responsible for reduction of the coercivity. The estimation of the critical diameter for single-domain behavior is 460 nm. The results also

Table 1
Magnetic properties of the samples with different pH values, Fe^{3+}/Sr^{2+} = 9, separated by filteration method and calcined at 750 °C for 2 h.

pH	M_s (emu/g)	H_c (Oe)	M_r
9	9.7	5231	5.6
11	38	5045	22.5
13	51	4733	28.5

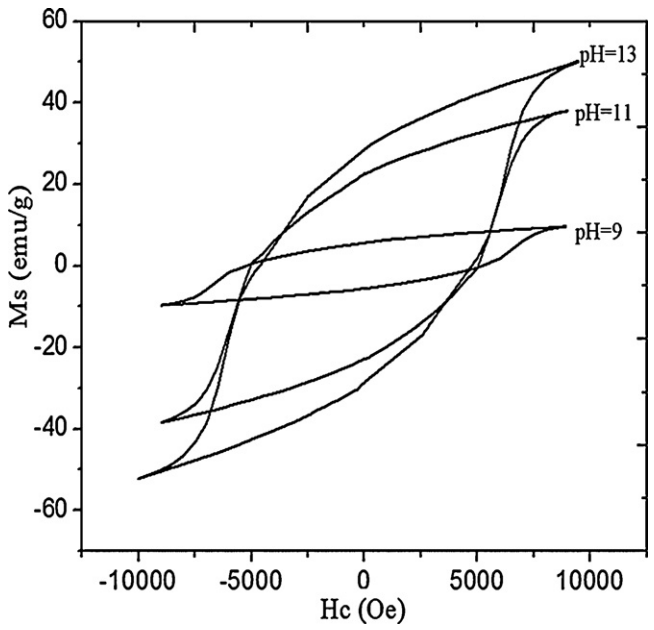

Fig. 11. Hysteresis curves of the samples synthesized at different pH values with Fe^{3+}/Sr^{2+} = 9, separated by filteration method and calcined at 750 °C for 2 h.

show an increase in the saturation magnetization with increasing of the pH. This is due to increase of strontium hexaferrite phase with pH [17]. The lower saturation magnetization of the samples in comparison with those reported in the literature [23] is due to insufficient applied magnetic field (10,000 Oe) and incomplete saturation of the samples.

Fig. 12 shows hysteresis curves of the samples synthesized with and without PVP at different Fe^{3+}/Sr^{2+} molar ratios and calcination temperatures. In the case of the samples prepared without PVP the saturation magnetization increased from 28.6 to 34.3 emu/g by decreasing the Fe^{3+}/Sr^{2+} molar ratio from 12 to 11. This may be attributed to the increase of strontium hexaferrite phase at lower Fe^{3+}/Sr^{2+} molar ratio. Decreasing the coercivity from 5583 Oe (at Fe^{3+}/Sr^{2+} = 12) to 5365 Oe (at Fe^{3+}/Sr^{2+} = 11) could be because of the reduction in particle size. The coercivity and the saturation magnetization of the produced strontium hexaferrite with 1 wt% PVP were 3724 (Oe) and 52.9 (emu/g), respectively. The lower coercivity of

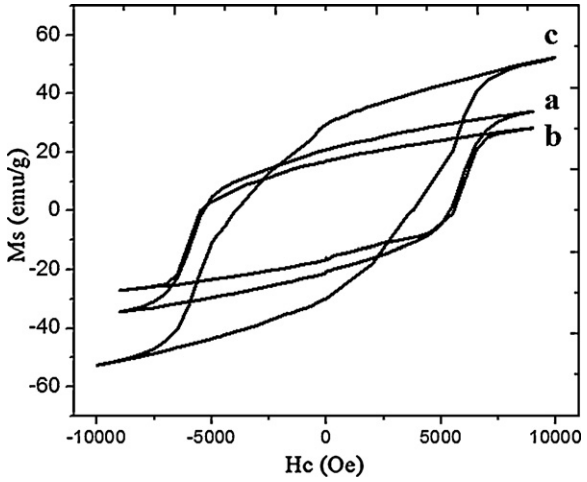

Fig. 12. Hysteresis curves of the samples precipitated at pH = 13 and separated by filteration method, (a) Fe^{3+}/Sr^{2+} = 11 after calcination at 750 °C for 2 h, (b) Fe^{3+}/Sr^{2+} = 12 after calcination at 750 °C for 2 h and (c) Fe^{3+}/Sr^{2+} = 9 after calcination at 700 °C for 2 h, in the presence of 1 wt% PVP.

the sample in comparison with the synthesized sample without PVP is due to its smaller average particle size [23].

4. Conclusion

1. The influences of pH, Fe^{3+}/Sr^{2+} molar ratio and using PVP on the phase composition, particle size and magnetic properties of strontium hexaferrite nanoparticles synthesized by coprecipitation method were investigated.
2. The results showed that the single-phase strontium hexaferrite could be synthesized in a mixture of the deionized water/ethanol (50/50) as the solvent at 800 °C.
3. The $SrFe_{12}O_{19}$ formation is promoted by increasing the pH from 9 to 13 and it increased the saturation magnetization of the samples.
4. Reduction of Fe^{3+}/Sr^{2+} molar ratio from 12 to 9 increased the amount of strontium hexaferrite phase and decreased the particle size. Accordingly, increasing the saturation magnetization and decreasing the coercivity can be explained.
5. The single-phase $SrFe_{12}O_{19}$ nanoparticles were synthesized at low temperature of 700 °C in the presence of 1 wt% PVP. The reduction in coercivity of the nanoparticles may result from the size reduction.

References

[1] O. Kubo, T. Ido, H. Jokoyama, IEEE Trans. Magn. 18 (1982) 1122–1124.
[2] X.X. Liu, J.M. Bai, F.L. Wei, Z. Yang, A. Morisako, M. Matsunori, J. Magn. Magn. Mater. 212 (2000) 273–275.
[3] M. Radwan, M.M. Rashad, M.M. Hessien, J. Mater. Process. Technol. 181 (2007) 106–109.
[4] S. Castro, M. Gayoso, C. Rodríguez, J. Mira, J. Rivas, S. Paz, M.J. Greneche, J. Magn. Magn. Mater. 140 (1995) 2097–2098.
[5] H.F. Yu, K.C. Huang, J. Magn. Magn. Mater. 260 (2003) 455–461.
[6] A. Ataie, M.R. Piramoon, I.R. Harris, C.B. Ponton, J. Mater. Sci. 30 (1995) 5600–5606.
[7] J.F. Wang, C.B. Ponton, I.R. Harris, J. Alloys Compd. 369 (2004) 170–177.
[8] J. Fang, J. Wang, L. Gan, S. Ng, J. Ding, X. Liu, J. Am. Ceram. Soc. 83 (2000) 1049–1055.
[9] G.M. Suarez, M.C. Morales, M.M. Guerrero, K.K. Jo-hal, H.M. Molinar, O.E. Valenzuela, J.I. Garcia, Mater. Chem. Phys. 77 (2003) 796–801.
[10] W. Zhong, W. Ding, N. Zhang, J. Hong, Q. Yan, Y. Du, J. Magn. Magn. Mater. 168 (1997) 196–202.
[11] W. Zhanyong, Z. Liuming, L. Jieli, F. Yougzheng, J. Magn. Magn. Mater. 322 (2010) 2782–2785.
[12] R. Muller, C. Ulbrich, W. Schuppel, H. Steinmetz, E. Steinbei, J. Eur. Ceram. Soc. 19 (1999) 1547–1550.
[13] S.E. Jacobo, M.A. Blesa, C. Domingo-Pascual, R. Rodriguez-Clemente, J. Mater. Sci. 32 (1997) 1025–1028.
[14] S.R. Janasi, M. Emura, F.J.G. Landgraf, D. Rodrigues, J. Magn. Magn. Mater. 238 (2002) 168–172.
[15] M.J. Iqbal, M.N. Ashiq, J. Chem. Eng. 136 (2008) 383–389.
[16] M.N. Ashiq, M.J. Iqbal, I.H. Gul, J. Magn. Magn. Mater. 323 (2011) 259–263.
[17] M.M. Hessien, M.M. Rashad, K. El-Barawy, J. Magn. Magn. Mater. 320 (2008) 336–343.
[18] D.H. Chen, Y.Y. Chen, Mater. Res. Bull. 37 (2002) 801–810.
[19] A. Davoodi, B. Hashemi, M.H. Yousefi, J. Magn. Magn. Mater. 323 (2011) 3054–3057.
[20] D. Lisjak, M. Drofenik, J. Eur. Ceram. Soc. 26 (2006) 3681–3686.
[21] S.R. Janasi, D. Rodrigues, F.J.G. Landgraf, M. Emura, IEEE Trans. Magn. 36 (2000) 3327–3329.
[22] B.D. Cullity, C.D. Graham, Introduction to Magnetic Materials, John Wiley & Sons Inc., Hoboken, New Jersey, 1972.
[23] H. Kojima, in: E.P. Wohlfarth (Ed.), A Handbook on the Properties of Magnetically Ordered Substances, North-Holland, Amsterdam, 1982.